Identification of Radicals and Determination of Their Yields in the Radiolytic Oxidation of Glycine. Time-resolved ESR Methodology

Gordon L. Hug* and Richard W. Fessenden

Radiation Laboratory, University of Notre Dame, Notre Dame, Indiana 46556−0579

Received: February 10, 2000; In Final Form: April 28, 2000

Both aminomethyl ($^{\bullet}CH_2NH_2$) and $H_2N-{}^{\bullet}CH-CO_2^-$ radicals were identified by time-resolved ESR spectroscopy in the oxidation of glycine anions by $^{\bullet}OH$. Previous ESR measurements had detected only the $H_2N-{}^{\bullet}CH-CO_2^-$ radical in these systems. The rise times of the ESR lines for these two different radicals are consistent with both of the radicals being formed in the initial reaction of $^{\bullet}OH$ with the glycine anions. The yields of these two C-centered radicals relative to the total yield of $^{\bullet}OH$ are approximately 29% for aminomethyl radicals and 53% for $H_2N-{}^{\bullet}CH-CO_2^-$ radicals. The yield of aminomethyl radicals from methlyamine was 53%. No ESR lines attributable to aminyl radicals could be directly detected in solutions of glycine ($HN^{\bullet}-CH_2-CO_2^-$) at high pH or low pH, or in solutions of methylamine ($HN^{\bullet}-CH_3$). However, clear evidence for the presence of the aminyl radicals was obtained in spin-trapping experiments using the *aci*-anion form of nitromethane with both methylamine and glycine. The rapid appearance of aminomethyl radicals in a complementary experiment with hydrated electrons reacting with *N*-chloroglycine could be simply explained on the basis of the formation of N-centered radicals in this situation. The ESR method for determining the yields was tested in the $^{\bullet}OH$ oxidation of methylamine and succinic acid. The implications of the findings of this work are discussed in the context of the recently proposed scheme for the oxidation of glycine anions by $^{\bullet}OH$.

Introduction

A revitalization of interest in the oxidation of amino acids has been stimulated by two separate areas of application. First, there has been intense research activity recently in oxidative stress[1] and the role of reactive oxygen species in aging.[2] The oxidation of glycine as the simplest amino acid could serve as a model for characterizing oxidations in complex natural systems. The second area in which the oxidation of glycine has been generating interest is in nuclear-waste cleanup.[3] Here, glycine serves as a model compound for complexants in nuclear-waste tanks. The ease and fate of radiolytic oxidation of these complexants are of practical interest in the cleanup efforts.

A recent paper[4] presented a systematic scheme for the oxidation of glycine anions by hydroxyl radicals ($^{\bullet}OH$) that were generated from the radiolysis of water. An abbreviated version of this mechanism is presented in Scheme 1. One goal in presenting this mechanism[4] was to reconcile the apparently contradictory observations that (1) only the presumably non-decarboxylating $H_2N-{}^{\bullet}CH-CO_2^-$ radical was observed by ESR in the steady-state radiolysis of glycine anions[5] whereas (2) large amounts of carbon dioxide were found in the gamma-radiolysis of glycine anions.[6] Other steady-state ESR experiments in basic aqueous solution using $TiCl_3-H_2O_2$ flow methods[7−11] and gamma-radiolysis[12] also reported no formation of the $^{\bullet}CH_2NH_2$ radicals that should accompany any CO_2 formation from the $^{\bullet}OH$ oxidation of glycine anions.

From Scheme 1, it can be seen that no $H_2N-{}^{\bullet}CH-CO_2^-$ radicals are formed in the initial oxidation of glycine anions by $^{\bullet}OH$. The initial radicals from this reaction are suggested[4] to be $H_2N^{\bullet+}-CH_2-CO_2^-$ and $HN^{\bullet}-CH_2-CO_2^-$. Scavenging experiments with methyl viologen, MV^{2+}, indicated that a reducing radical was produced very rapidly.[4] Because it appeared to quantitatively corroborate the decarboxylation yields, this reducing radical was assigned as the aminomethyl radical, $^{\bullet}CH_2NH_2$, which was formed when the zwitterion radical, $H_2N^{\bullet+}-CH_2-CO_2^-$, decarboxylated. The rest of the mechanism involves protonations whereby the aminyl radical, $HN^{\bullet}-CH_2-CO_2^-$, is protonated slowly by the secondary processes that form the zwitterion radical, $H_2N^{\bullet+}-CH_2-CO_2^-$, and hence, more carbon dioxide.[4]

SCHEME 1: Oxidation of Glycine (Anionic Form)

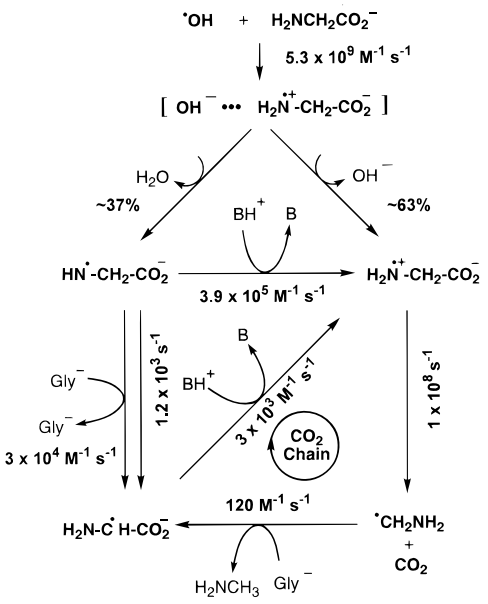

The evidence for the various radicals presented in Scheme 1 was inferential.[4] Scavenging reactions[4] for reducing radicals

10.1021/jp000533u CCC: $19.00
Published on Web 07/06/2000

using MV^{2+} or ferricyanide and scavenging reactions[4] for oxidizing radicals using hydroquinone left open questions about the detailed assignment of the radicals actually being scavenged. The oxidizing radicals scavenged in pulse radiolysis experiments were suggested to be $HN^{\bullet}-CH_2-CO_2^-$, and all of the reducing radicals, which were scavenged in the faster of two observed growth processes, were suggested to be $^{\bullet}CH_2NH_2$.[4] These assignments of radicals were in some doubt as only the $H_2N-{}^{\bullet}CH-CO_2^-$ radical was seen directly in in situ ESR[5] and spin-trapping experiments[12] in steady-state, radiolytic oxidations of glycine anions. However, the latter work[12] also identified $^{\bullet}CO_2^-$ -type spin adducts at pH 11. Because a complete set of rate constants for the various reactions in Scheme 1 was estimated,[4] it is possible to simulate the time-dependent concentrations of these radicals and to see that time-resolved ESR (TRESR) techniques can be used to search for direct evidence at short times following the radiolysis pulse. The purpose of the current work is to use time-resolved ESR spectroscopy to look for evidence of the radicals proposed in Scheme 1 and to see if their yields and time profiles match those inferred from the proposed scheme.

Experimental Section

Glycine, sodium hypochlorite, and methylamine were purchased from Aldrich. Anhydrous sodium sulfite was obtained from Mallinckrodt, succinic acid from J. T. Baker Chemical, and potassium hydroxide and *tert*-butyl alcohol from Fisher Scientific. Nitromethane (99%) was purchased from Aldrich. All of these chemicals were used without further purification. *N*-chloroglycine was prepared in situ as described below. The deionized water was purified in a reverse osmosis/deionization system from a Serv-A-Pure Co. There is a UV-irradiation unit in the circulating section of this water-purification system.

The in situ time-resolved ESR equipment was described previously.[13−15] The Van de Graaff accelerator supplied 2.8-MeV electron pulses of approximately 1-μs duration to the flowing aqueous solutions. The quartz cell of 0.4-mm thickness was irradiated edge-on. The solution passed through a heat-exchange unit before entering the ESR cell to cool the solution before irradiation so that bubbles from the N_2O could be avoided. The measurements were made at a temperature of about 288 K. Most of the experiments were done in N_2O-saturated solutions where hydrated electrons, e_{aq}^-, are rapidly converted into $^{\bullet}OH$ by the reactions

$$H_2O \rightsquigarrow e_{aq}^-, {}^{\bullet}OH, H, H^+ \qquad (1)$$

$$e_{aq}^- + N_2O \rightarrow N_2 + O^{\bullet -} \qquad (2)$$

$$O^{\bullet -} + H_2O \rightleftharpoons {}^{\bullet}OH + OH^- \qquad pK_a = 11.9 \qquad (3)$$

The radiation doses and corresponding initial radical concentrations could be varied by adjusting the electron-beam current. Typical conditions corresponded to a concentration of hydroxyl radicals, $^{\bullet}OH$, in the N_2O-saturated solutions in the range of 40−50 μM, although some experiments were performed at lower concentrations. As usual, the ESR signals are proportional to the population differences of the spin levels once the spins have had time to relax in the magnetic fields.[16] The signal-averaged kinetic data are accumulated by summing pairs of matched traces. One trace in each pair is acquired at the nominal external magnetic field, while its partner is acquired at an external magnetic field that is shifted by current through coils on the cavity to a position in the spectrum where no transition is located. These on- and off-resonance traces are subtracted, and the procedure is repeated with each intermediate result being folded into the average. This signal-averaging procedure was repeated typically 400 times per trace for relatively strong ESR signals, but typically 800 times per trace, and even 1600, for the weaker signals. The accumulation of individual traces occurs at 100 per second, so care was taken that the solution flow was fast enough to avoid product buildup. The solution flow rate was typically 20 $cm^3\ min^{-1}$. In the region near the ESR line of the silica cell, it was necessary to take a blank trace for subtraction as the cell does show a weak transient signal.

The boxcar-scanning mode of operation of the ESR spectrometer has also been described previously.[13] Because the N-centered radical, $HN^{\bullet}-CH_2-CO_2^-$, was not known except in single crystals with no report of a g factor,[17] it was necessary to scan through the spectrum in most of these systems to search for the lines. In this mode, the data acquisition is done by continually stepping the magnetic field between two fields separated by about one ESR line width. The data consist of the amplitude difference between traces over a selected time interval. A number of data values are averaged and sent through a DA converter to a strip chart recorder. The external magnetic field is slowly scanned through a range to display a spectrum that has a first-derivative form.

The steady-state or continuous mode of ESR radiolysis experiments used the same spectrometer,[15] but with a different cavity, with field modulations at 100 kHz and 200 Hz, and with tandem synchronous detectors in the signal channel. A second-derivative presentation is obtained. Irradiation used a similar average beam current of about 2−5 μA and similar solution flow rates.

Methodology

The yields of the radicals were estimated by comparing the ESR signals from the radicals with that from the $SO_3^{\bullet -}$ radical (produced from 5 mM SO_3^{2-}) as the standard for 100% yield of $^{\bullet}OH$ in N_2O-saturated aqueous solutions. The basic principle is to compare the areas of the ESR lines. However, it is necessary to take into account a number of factors, such as the effect of the chemical decay and time constant, so that an extrapolated, or initial, amplitude can be determined. A better approach seemed to be to model the ESR time responses and to compare the amplitudes of those curves. The calculated curves take into account the line width through the field inhomogeneity (ΔB_0) and T_2 value, any saturation of the signal, as well as the time constant and decay rate.

The time profile of an ESR signal was calculated using modified Bloch equations, as described previously.[13] The set of differential equations included the usual Bloch description of the magnetic response for the three components of magnetization in the rotating reference frame and a separate equation for the radical decay by bimolecular reaction. (Because of a somewhat limited signal-to-noise ratio in the data, a rather simple second-order decay model based on the total radical concentration was used.) The equations were integrated numerically with an initial condition of Boltzmann equilibrium. (The rate of the $^{\bullet}OH$ reaction with the solute was sufficiently fast that it was not usually necessary to include the radical-formation reaction. The electron spins of radicals produced from $^{\bullet}OH$ are in Boltzmann equilibrium as a result of very rapid relaxation in that radical.)

The magnetic-field inhomogeneity (ΔB_0) was included by integrating the Bloch equations for separate "spin packets" at different field offsets from exact resonance. The responses were

then combined with a Gaussian weighting function, with $2.345\sigma = \Delta B_0$; the magnetic-field inhomogeneity was determined as described below. The instrumental time constant (usually 0.9 μs, but 0.35 μs for strong signals) was applied through a final differential equation that also modeled a 1-μs blank-out period following the radiolysis pulse when a microwave switch between the cavity and the detector was turned off. The ESR time dependence so calculated was compared with the observed signal, and a scaling factor was determined for multiplying the amplitude of the calculated curve for the best fit. The value of this scaling factor for a given ESR line relative to that for the $SO_3^{\bullet-}$ reference served (after inclusion of the appropriate statistical weighting factor for the number of splittings) to measure the radical yield.

The usual approach was to fit the ESR time curve for $SO_3^{\bullet-}$ by adjusting the scaling factor and concentration to fit the amplitude and decay with a value of the second-order decay rate constant of 1×10^9 M^{-1} s^{-1}. (This value is approximately correct, and the exact value is not important for the relative yield measurements.) The values of the other parameters were determined by the methods described below. The consistency of the method is indicated by the fact that, over an extended time period of several months and with the same ESR cavity and cell, the scaling factor for $SO_3^{\bullet-}$ varied only between 9.5 and 11.4. The transient response for the ESR line of the radical under study was then fit by setting the radical concentration according to the electron beam collected on the ESR cell and adjusting the scale factor for the calculated curve.

A number of parameters in this calculation had to be evaluated. These include the magnetic-field inhomogeneity (ΔB_0), the microwave magnetic-field amplitude (B_1), the T_1 and T_2 spin-relaxation times for the radical of interest, and the concentration of $^{\bullet}$OH produced by the pulse. In addition, the chemical-decay behavior of the radical must be accounted for, and any chemically induced electron polarization (CIDEP) had to be considered. Once these parameters are known, a reliable prediction of the time profile can be made.

The magnetic-field inhomogeneity, ΔB_0, and the microwave magnetic-field amplitude, B_1, were determined separately using the $^-O_2CCH{=}C^{\bullet}CO_2^-$ radical. This radical has reported relaxation times of $T_1 = 9$ μs and $T_2 = 7$ μs[14] and is formed from reaction of both H$^{\bullet}$ and e_{aq}^- (with rapid protonation of the anion radical by water) with acetylenedicarboxylic acid dianion in radiolysis experiments. The two units of negative charge reduce the chemical-decay rate. Because of CIDEP in H$^{\bullet}$ before the addition reaction, the initial magnetization of the high-field line is about 2 times the Boltzmann value, so that good transient (Torrey) oscillations are developed. The microwave-field amplitude, B_1, is obtained by fitting the frequency of the transient oscillations, and the damping of the oscillations allows a determination of T_2 for the $^-O_2CCH{=}C^{\bullet}CO_2^-$ radical. Comparison of the long-time amplitude of the signal at several microwave-power levels allows T_1 to be determined. The values so determined for the $^-O_2CCH{=}C^{\bullet}CO_2^-$ radical were $T_1 = 16$ μs, $T_2 = 7$ μs, and $B_1 = 0.027$ G at a power setting of -10 dB. This value of B_1 was used in other computations; it is listed in Table 1.

The magnetic-field inhomogeneity, ΔB_0, at the sample position in the cavity was determined from the width of a line in the $^-O_2CCH{=}C^{\bullet}CO_2^-$ spectrum. In this work, line widths were measured using a point-by-point method. Kinetic traces in the vicinity of the line were recorded, and a line shape could be produced from the various amplitudes (each measured at a sufficiently long time that any transient behavior of the spin system had decayed). An ESR line, so generated, was then fit by a Lorentzian function, from which the *experimental* width at half-height could be determined. ESR lines constructed by this method are shown in Figure 1 for several of the radicals involved. The experimental width of the high-field line of $^-O_2CCH{=}C^{\bullet}CO_2^-$ was used to obtain the external magnetic-field inhomogeneity, ΔB_0, by comparison with a theoretical width calculated from $\int g(B_0 - B)\, f(B - B_0)\, dB$. In this expression, $g(B_0 - B)$ is the contribution to the ESR amplitude from that part of the sample with an actual field of B when the nominal field is B_0. This function is a theoretical line shape computed from the standard[18] steady-state magnetic resonance amplitude using the previously determined values of T_1, T_2, and the microwave field, B_1. The other factor, $f(B - B_0)$, is proportional to $\exp\{-[2.345(B - B_0)/\Delta B_0]^2/2\}$, namely, it is a Gaussian profile, centered on the nominal external magnetic-field, B_0, and its width is a measure of the magnetic-field inhomogeneity at the sample. The theoretical width of the line computed from the integral expression was made to fit the experimental line width by varying the width parameter (full width at half-height, ΔB_0) of the field inhomogeneity. A value of $\Delta B_0 = 0.037$ G was found and is listed in Table 1. This value for the external magnetic-field inhomogeneity was used in all subsequent calculations. With this inhomogeneity parameter established, the above integral expression was used to compute the T_2 values for the other radicals by a similar procedure of matching experimental line widths with the theoretical values computed from the integral formula. Parameters for the radicals of concern are given in Table 1.

The radicals to be studied are reactive and show chemically induced dynamic electron polarization (CIDEP) by the radical-pair mechanism. The low-field lines are in emission (E) at microsecond times, and the high-field lines are in enhanced absorption (A). This E/A pattern is the normal one seen when

TABLE 1: Parameters Used in Modeling ESR Responses

radical	T_1[a]	T_2[a]
$SO_3^{\bullet-}$	1.5	1.5
$^-O_2CCH{=}C^{\bullet}HCO_2^-$	16	7
$^-O_2CCH_2C^{\bullet}HCO_2^-$	3.8	1.4
$^{\bullet}CH_2NH_2$	1.4	1.4
$H_2N{-}^{\bullet}CH{-}CO_2^-$	1.4	1.4
inhomogeneity parameter, ΔB_0	0.037 G	
microwave magnetic field, B_1	0.027 G at -10 dB	

[a] Values in microseconds.

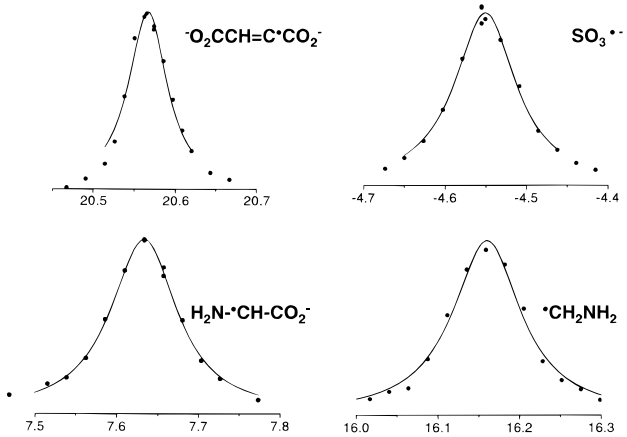

Figure 1. ESR line shapes determined by the point-by-point method. The amplitude corresponds to the average level of the transient response in a time window 10 μs or more after the formation pulse. The horizontal axis represents magnetic field in gauss from a position defined by $g = 2.000\,43$.

singlet radical-pairs react so that triplet pairs remain. The observed ESR line amplitudes will be modified by this polarization and so will not correspond with Boltzmann population of the spin levels. Consequently, these amplitudes will not quantitatively represent the concentration. To take this effect into account, the time profile of lines symmetrically located in the spectrum were recorded and averaged. The positive polarization for the high-field line will be compensated by the negative polarization of the low-field line. If there are two different radicals with different g factors and cross reactions between them, then this procedure is only approximate. The results to be given for several pairs of lines at different separations from the center of the spectrum show good agreement, so any error introduced by this approach is small.

The microwaves to the detector are gated off for approximately 1 μs while the electron beam is on. The rise times of the microwave signals are related to the formation rate of the radicals, but in addition, there is a natural response time of the spins, corresponding to the time for the macroscopic magnetic moment to rotate away from the direction of the external magnetic field, B_0.[16] This time is determined by the strength of the microwave magnetic field, B_1. The initial part of the signal is also distorted from a true concentration profile by some saturation effects. All of these effects are accounted for in the Bloch-equation modeling. The calculated kinetic curves also account for the electron beam pulse width and microwave gating, and unless otherwise mentioned, the radicals were assumed to be formed rapidly (in a time considerably <1 μs) after formation of $^{\bullet}$OH radicals as appropriate for the known reaction rates.

Simulations for Glycine. Because the reaction mechanism for glycine, Scheme 1, is complex, it was advisable to predict the expected behavior so that optimum conditions for observation of the aminyl radical, $HN^{\bullet}-CH_2-CO_2^-$, could be found. In the recent work,[4] rate constants were measured, estimated, or taken from the literature for all of the processes in Scheme 1. The listed rate constant of 3.9×10^5 M^{-1} s^{-1} for the protonation of the aminyl radical is the value when the proton donor BH^+ is the glycine zwitterion.[4] From the values listed in Scheme 1, it is possible to get a rough quantitative picture of the expected time development of the radical concentrations following a radiolysis pulse. Analytic solutions were not attempted as nonlinear equations were expected because of radical−radical reactions at the higher doses and concentrations. The kinetics were simulated by a stochastic method that was available from IBM on the Internet.[19] The radical−radical rate constants were not determined for the scheme. The values used for the simulation were 2.5×10^9 M^{-1} s^{-1} for oxidizing radical-reducing radical rate constants, 2×10^9 M^{-1} s^{-1} for reducing radical-reducing radical rate constants, and 1×10^8 M^{-1} s^{-1} for oxidizing radical-oxidizing radical rate constants.

Conditions were sought in which the aminyl radical, $HN^{\bullet}-CH_2-CO_2^-$, would be the most prominent, namely, having a sufficiently long lifetime to be observed in the ESR experiment and also being present in a sufficient yield. One of the conditions where these requirements are met is at pH 10.6 with 100 mM glycine. The simulation is shown in Figure 2. These conditions are significant for the following reasons. (1) pH 10.6 is 1 pH unit above the pK_a of the glycine zwitterion so that 90% of glycine is in the anionic form. $^{\bullet}$OH reacts faster, by over 2 orders of magnitude, with the anion than with the zwitterionic form of glycine. This pH ensures that intereference by radicals from the zwitterion should be at a minimum. (2) pH 10.6 is roughly 1 pH unit below the pK_a of $^{\bullet}$OH so the $O^{\bullet-}$ radical should also

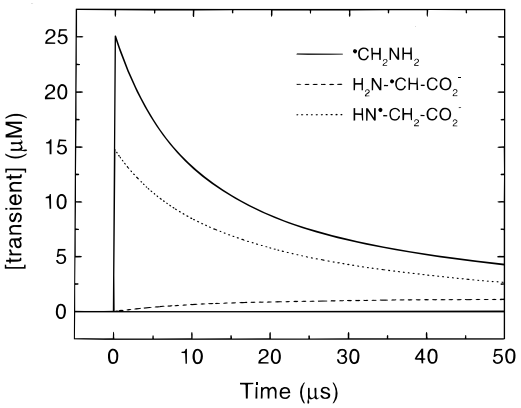

Figure 2. Stochastic simulation of the kinetics in Scheme 1 for a 100 mM glycine, N_2O-saturated aqueous solution, pH 10.6, and a dose corresponding to an initial [$^{\bullet}$OH] = 40 μM.

be a minor competitor for glycine. (3) Most important of all is that the N-centered radical is expected to be relatively long-lived, see Figure 2. This is because of the relatively slow conversion into its protonated form $H_2N^{\bullet+}-CH_2-CO_2^-$, which is expected to decarboxylate immediately.[20]

Results and Discussion

Two types of time-resolved ESR experiments were performed. First, transient traces were taken in the neighborhood of field offsets of the known ESR transitions of radicals that were expected to be present. Second, substantial ranges of the field offsets were scanned with the instrument operating in the boxcar mode in order to measure ESR signals in a fixed time interval following the radiolysis pulse. The boxcar mode allowed fairly rapid exploration for the unknown position of the lines of the aminyl radical, $HN^{\bullet}-CH_2-CO_2^-$, or any other species. On the other hand, the kinetic traces permitted a detailed comparison to the predictions of the kinetic scheme,[4] allowed for a detailed construction of the line shapes (as in Figure 1), and formed the basis for the yield determinations discussed in the Methodology section.

Succinate Radicals. As an initial test of the methodology, the oxidation of succinate dianions by $^{\bullet}$OH was used for calculating the yields of radicals. The dianion, $^-O_2C-CH_2-CH_2-CO_2^-$, of succinic acid can form only one type of radical following H abstraction by $^{\bullet}$OH, namely, $^-O_2C-{}^{\bullet}CH-CH_2-CO_2^-$. Decarboxylation is not expected to be a viable reaction, but the reaction with $^{\bullet}$OH is somewhat slower, 7.6×10^8 M^{-1} s^{-1},[21] than the corresponding reaction with SO_3^{2-}, 5.1×10^9 M^{-1} s^{-1}.[22] The average of the symmetrically located pair of lines closest to the center of the spectrum was used. From Table 2, it can be seen that the yield of $^-O_2C-{}^{\bullet}CH-CH_2-CO_2^-$ at pH 10, in two determinations, averages to nearly 100%. It is estimated that the expected error in this measurement is about 5−10%. It can also be noted there was no evidence of decarboxylation because no ESR line attributable to $^{\bullet}CH_2-CH_2-CO_2^-$ was seen in the center of the spectrum where one is expected.[23]

Aminomethyl Radicals from Methylamine. The methods described above were next applied to the oxidation of methylamine by $^{\bullet}$OH. This was of interest for two reasons. First, it presented a somewhat simpler case than glycine in that decarboxylation could not occur. Second, it gave the opportunity of applying the methodology for measuring yields without interference from the overlapping of several spectra because only ESR lines from aminomethyl radical, $^{\bullet}CH_2NH_2$, were observed.

TABLE 2: Data for Reaction Yield Determinations

radical	lines	μwave power	scale factor[a]	degen-eracy	%
Reaction: $^{-}O_2CCH_2CH_2CO_2^{-} + {}^{\bullet}OH$ (pH 10.0)					
$SO_3^{\bullet-}$	center	−15 dB	10.7	1	100
$^{-}O_2CCH_2C^{\bullet}HCO_2^{-}$	±13.45 G	−15 dB	1.395	1/8	104
		−15 dB	1.23	1/8	92
Reaction: $H_3CNH_2 + {}^{\bullet}OH$ (pH 10.7)					
$SO_3^{\bullet-}$	center	−15 dB	11.4	1	100
$^{\bullet}CH_2NH_2$	center[b]	−15 dB	0.52	4/48	55
	±9.54 G[b]	−10 dB	0.23	2/48	48
	±9.54 G[b]	−15 dB	0.24	2/48	50
	±15.68 G	−10 dB	0.14	1/48	59
Reaction: $H_2NCH_2CO_2^{-} + {}^{\bullet}OH$ (pH 10.6)					
$SO_3^{\bullet-}$	center	−10 dB	10.4	1	100
$H_2N-{}^{\bullet}CH-CO_2^{-}$	−0.50 G	−10 dB	0.21	1/24	48
	±7.10 G	−10 dB	0.26	1/24	60
	±12.70 G	−10 dB	0.24	1/24	55
	±13.20 G	−10 dB	0.22	1/24	51
$^{\bullet}CH_2NH_2$	±9.54 G[b]	−10 dB	0.113	2/48	26
	±15.68 G	−10 dB	0.070	1/48	32

[a] Factor multiplying calculated curve to make it fit the observed curve. [b] These lines have a second-order splitting into two lines, and the scale factor has been corrected for the effect of the incomplete overlap.

TABLE 3: ESR Parameters for Radicals from Methylamine and Glycine[a]

radical	a_H(CH)	a_N	a_H(NH)	g
$^{\bullet}CH_2NH_2$	15.35(2)	4.93	4.60(2)	2.002 89
$H_2N-{}^{\bullet}CH-CO_2^{-}$	13.70	6.10	3.39, 2.90	2.003 47

[a] All splittings in gauss.

A search was made for ESR lines with methylamine at pH 10.6. The lines found were all consistent with the known spectrum and parameters of aminomethyl. The isotropic hyperfine coupling constants were determined from these lines to be a_H(CH) = 15.35 G, a_H(NH) = 4.60 G, and a_N = 4.93 G. These couplings are close to the previously reported values.[5] The g factor is 2.002 89. (See Table 3 for the parameters observed here.) No other lines could be seen in a spectrum taken with the boxcar mode. Time-resolved traces of ESR amplitude were taken for a number of the lines in this spectrum. Data for the central line and for a symmetrically located pair of lines is shown in Figure 3. From Table 2, it can be seen that the methodology for determining the yield was applied for the single, central line (Figure 3b), which should be unpolarized, and for the average of high- and low-field lines of two symmetrically located pairs of lines (Figure 3a). In addition, the lines at ±9.54 G of the center of that spectrum were used for yield determinations at two different microwave powers. The agreement between all of these determinations is quite good.

The yield of 53% (average) is of interest in that, clearly, there is another radical produced that is not detected by ESR at this sensitivity. We propose that the radical $HN^{\bullet}-CH_3$ is also present to the extent of about 47% of the $^{\bullet}OH$ yield and that the ESR lines are too broad to be readily detected. It should be noted that the spin-trapping experiments described below do show this radical to be present. This radical is expected to have somewhat broadened lines because it has only two heavy atoms (compared to hydrogen), and thus, a rapid rotation about the C−N bond axis can produce spin relaxation by spin−rotation coupling. The radical $HN^{\bullet}-CH_3$ was proposed as being present in systems of the type investigated here,[24] and it is known from irradiated solids.[25]

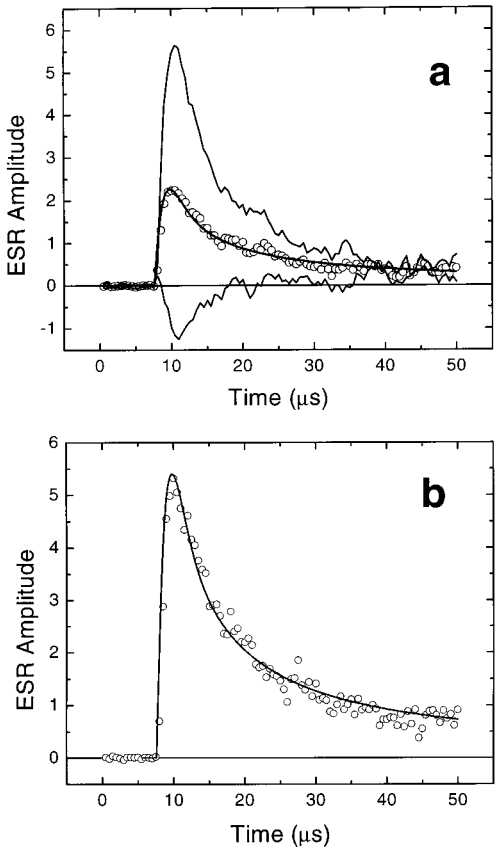

Figure 3. Transient ESR responses for $^{\bullet}CH_2NH_2$ in 10 mM methylamine solution at pH 10.7: (a) lines at ±9.54 G from the center at the spectrum (solid lines) and their average (open circles) with the simulated curve (smooth line); (b) the response of the center line and the simulated curve. The curves for the individual lines in the upper portion show CIDEP of the E/A type.

Glycine at High pH: Aminomethyl Radical. Boxcar field scans of irradiated N_2O-saturated, aqueous solutions of glycine at pH 10.6 showed lines from only $H_2N-{}^{\bullet}CH-CO_2^{-}$ and $^{\bullet}CH_2NH_2$ radicals. In particular, lines were present at all positions expected for $^{\bullet}CH_2NH_2$, so the identification is certain. It also revealed that many lines of the $H_2N-{}^{\bullet}CH-CO_2^{-}$ radical were overlapped by lines from $^{\bullet}CH_2NH_2$, particularly near the center of the spectrum. As a consequence, the measurements of radical concentration had to use symmetrically located line pairs. (This is the main reason the method was tested with methylamine.) A section of the spectrum that allows separation of the lines of the two species is given in Figure 4a. Lines of the two species showed the normal E/A polarization.

One of the kinetic traces that is characteristic of the aminomethyl radical is shown in Figure 5a for a 10 mM solution of glycine at pH 10.6. The data represent the average of the lines at ±9.54 G from the center of the spectrum for $^{\bullet}CH_2NH_2$. In Figure 5b is shown a corresponding trace for the lines of $H_2N-{}^{\bullet}CH-CO_2^{-}$ at ±12.70 G in that spectrum. The lifetime of $^{\bullet}CH_2NH_2$ is somewhat shorter than that of the concentration profile in the simulation of Figure 2. The short lifetime is likely due to the radical−radical reactions under the high doses from the Van de Graaff generator. It is also evident that the decay of $^{\bullet}CH_2NH_2$ is faster than that of $H_2N-{}^{\bullet}CH-CO_2^{-}$ in Figure 5b. The rate constant ($2k$) necessary to fit the decay was about 4 times as large for $^{\bullet}CH_2NH_2$ as for $H_2N-{}^{\bullet}CH-CO_2^{-}$ (about 4×10^9 M^{-1} s^{-1} as compared with 1×10^9 M^{-1} s^{-1}). We note that the faster decay of $^{\bullet}CH_2NH_2$ is not the result of its reacting

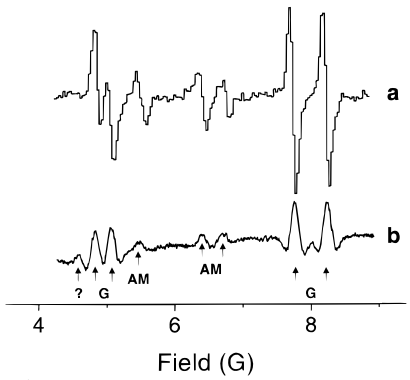

Figure 4. Partial spectra taken during radiolysis of an N_2O-saturated solution of 10 mM glycine at pH 10.7: (a) boxcar-mode scan during pulse radiolysis representing the average amplitude in the window 4−12 μs after the start of the electron pulse; (b) second-derivative scan taken during continuous radiolysis. Lines of $^{\bullet}CH_2NH_2$ are designated "AM", those of $H_2N-{}^{\bullet}CH-CO_2^-$ by "G", and an unknown line by "?".

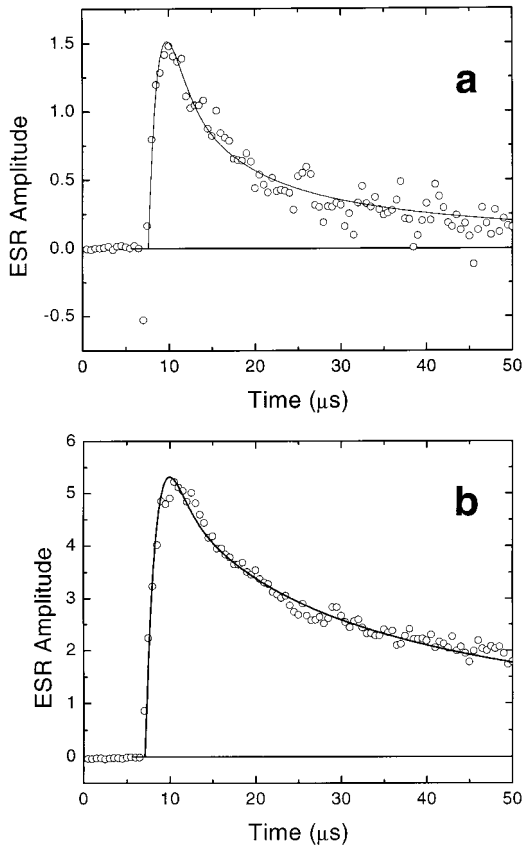

Figure 5. Transient ESR spectrum obtained in the irradiation of N_2O-saturated 10 mM glycine solution at pH 10.6: (a) average (open circles) of the lines of aminomethyl radical at ±9.54 G from the center of that spectrum; (b) average (open circles) of the lines of $H_2N-{}^{\bullet}CH-CO_2^-$ at ±12.70 G from the center of that spectrum. Entries corresponding to these simulated curves are presented in Table 2.

with glycine anion, as the decay was not significantly different at a concentration of 100 mM glycine.

Of particular note is the fast rise of the signals in Figure 5. The agreement of the rate of the initial signal rise with the calculated curve shows that the radicals are formed in considerably less than 1 μs. This rate is consistent with formation of the aminomethyl radical by a fast decarboxylation following the reaction of $^{\bullet}OH$ with the glycine anions, such as that in Scheme 1.

The yield of the $^{\bullet}CH_2NH_2$ radical was determined using the methodology described above. The result from averaging the matched lines, such as the average trace in Figure 5a, gives yields of 26% and 32% (average 29%, see Table 2) for two different pairs of matched lines.

The formation of aminomethyl radical was not reported in the previous steady-state in situ radiolysis[5] or in gamma-radiolysis, spin-trapping experiments at high pH.[12] The shorter lifetimes of the aminomethyl radicals and slightly larger ESR line widths, as compared with those of $H_2N-{}^{\bullet}CH-CO_2^-$, would discriminate against that radical in steady-state experiments that use second-derivative presentation. With this in mind, steady-state experiments on glycine were repeated here with a higher field modulation amplitude (≈150 mG), and lines of aminomethyl actually were seen (see Figure 4b). The previous failure to detect aminomethyl radicals in the steady-state in situ radiolysis experiments[5] was presumably the result of using a smaller field modulation and limited signal-to-noise ratio. (Possible very weak lines at the same positions as displayed here can be seen in this earlier work.)[5]

Glycine at High pH: $H_2N-{}^{\bullet}CH-CO_2^-$ Radicals. In addition to the lines assigned to aminomethyl radical, ESR lines were detected at field offsets characteristic of $H_2N-{}^{\bullet}CH-CO_2^-$ radicals (see Figure 4). The hyperfine coupling constants corresponding to these field offsets were determined to be $a_H(NH') = 3.39$ G, $a_H(NH'') = 2.90$ G, $a_H(CH) = 13.70$ G, and $a_N = 6.10$ G, and the g factor was determined to be 2.003 47 (see Table 3). These coupling constants were the same as the previously reported values for $H_2N-{}^{\bullet}CH-CO_2^-$ radicals.[5] The transitions are polarized in an E/A pattern similar to that observed for the aminomethyl radicals under the same conditions.

A kinetic trace, synthesized from the average of high- and low-field lines, for $H_2N-{}^{\bullet}CH-CO_2^-$ is shown in Figure 5b. The lines were at ±12.70 G from the center of that spectrum. The yield of $H_2N-{}^{\bullet}CH-CO_2^-$ computed from this trace was calculated to be 55% of the $^{\bullet}OH$ (see Table 2). The average for several measurements using various pairs of lines was 53%. The yield of $H_2N-{}^{\bullet}CH-CO_2^-$ computed from these traces was greater than the yield of aminomethyl radicals in the glycine-anion radiolysis. As was found for aminomethyl radicals, the rise time of the calculated curves indicates that the radicals were formed in considerably less than 1 μs.

Search for $HN^{\bullet}-CH_2-CO_2^-$. The other 18% (or 37%)[4] of the initial radicals formed in the reaction of $^{\bullet}OH$ with glycine anions was thought[4] to be the aminyl radical, $HN^{\bullet}-CH_2-CO_2^-$. These radicals have been discussed,[26] and there is some information about them in glycine crystals.[17] They were not directly observed in this work, but the deficit in ESR yield of the two C-centered radicals compared to the $^{\bullet}OH$ yield is not inconsistent with the inference of the existence of $HN^{\bullet}-CH_2-CO_2^-$ radicals from the experiments that used hydroquinone to scavenge oxidizing radicals.[4] As in the case of methylamine, the spin-trapping experiments shown below establish the presence of this aminyl radical.

A search for the direct display of ESR lines from this radical was desired. From Figure 2, it can be seen that pH 10.6 is a reasonable pH for observing quite long-lived aminyl radicals if this feature of the recent scheme is correct.[4] However, the spectral scans with the 10 mM and 100 mM glycine solutions at pH 10.6 showed no lines that could not be accounted for by either aminomethyl or $H_2N-{}^{\bullet}CH-CO_2^-$. This situation is analogous to that for methylamine. The $HN^{\bullet}-CH_2-CO_2^-$ must

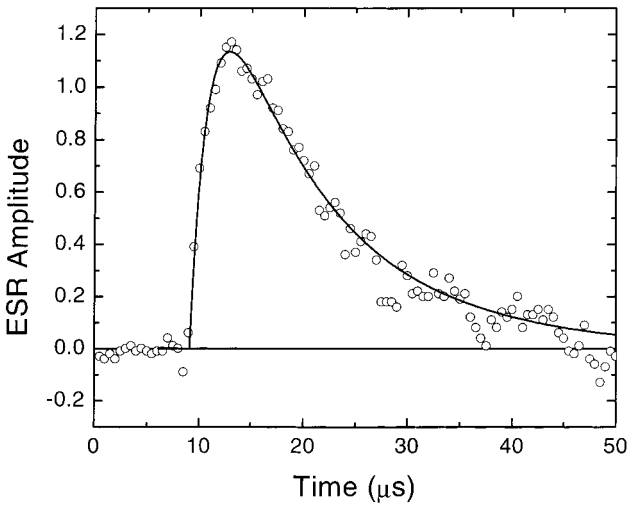

Figure 6. Transient ESR spectrum of $^{\bullet}CH_2NH_2$ in a solution of *N*-chloroglycine, see text.

have broad lines or a short lifetime if it is responsible for the missing radical yield.

To attempt to demonstrate that $HN^{\bullet}-CH_2-CO_2^-$ radicals really are present, another chemical preparation was employed. Nitrogen-centered radicals can be generated directly by the reaction of hydrated electrons with compounds containing nitrogen−chlorine bonds followed by subsequent elimination of chloride ions.[27] The nitrogen−chlorine bonds can be formed quantitatively by using HOCl to chlorinate the nitrogen.[28] In this case, NaOCl was diluted to about 3 mM and neutralized with approximately 3 mM of NaH_2PO_4. Excess glycine was added (approximately 4.5 mM) to form the *N*-chloroglycine. The resulting solution of pH 5.8 was saturated with nitrogen and irradiated in the ESR cavity. The boxcar mode was used to scan through an extensive section of the high-field side of the spectrum. No lines attributable to the $HN^{\bullet}-CH_2-CO_2^-$ radical could be found. The only lines found were some relatively weak lines from aminomethyl radical. The time-resolved mode was used to record the kinetic trace of one of these lines in Figure 6. To fit the rise of this curve it was necessary to include a relatively rapid formation rate of $4 \times 10^5\ s^{-1}$. The experiment was not repeated at a more basic pH because the stability of the *N*-chloroglycine in basic solution was thought to be a problem.

Glycine at Low pH. To make sure that nothing unexpected is happening at low pH that would obviate the above conclusions, ESR experiments were done on N_2O-saturated solutions of 100 mM glycine in the pH range 5.3−5.4. These high glycine concentrations were used in anticipation of a slow formation of radicals on the basis of the reported rate constants for the reaction of $^{\bullet}OH$ with glycine zwitterions.

Somewhat surprisingly, aminomethyl radicals are detected here also. The growth of the signal is consistent with the slow reaction of $^{\bullet}OH$ with glycine zwitterions. Also, there are small amounts of $H_2N-{}^{\bullet}CH-CO_2^-$. The intensity of the ESR lines of $H_2N-{}^{\bullet}CH-CO_2^-$ relative to that of aminomethyl radical lines is strikingly smaller than the corresponding ratio at pH 10.6. In addition to these signals, ESR lines can be seen that are roughly comparable in intensity to those of the aminomethyl radical signals. These new lines are at positions[7] consistent with a protonated form, namely, $H_2N-{}^{\bullet}CH-CO_2H$. The ratio of ESR line intensities for $H_2N-{}^{\bullet}CH-CO_2^-$ relative to $H_2N-{}^{\bullet}CH-CO_2H$ is somewhat greater than one would expect from the value $pK_a(H_2N-{}^{\bullet}CH-CO_2H) = 6.66$.[11] No lines were unaccounted for in the scans that could be attributed to aminyl radicals.

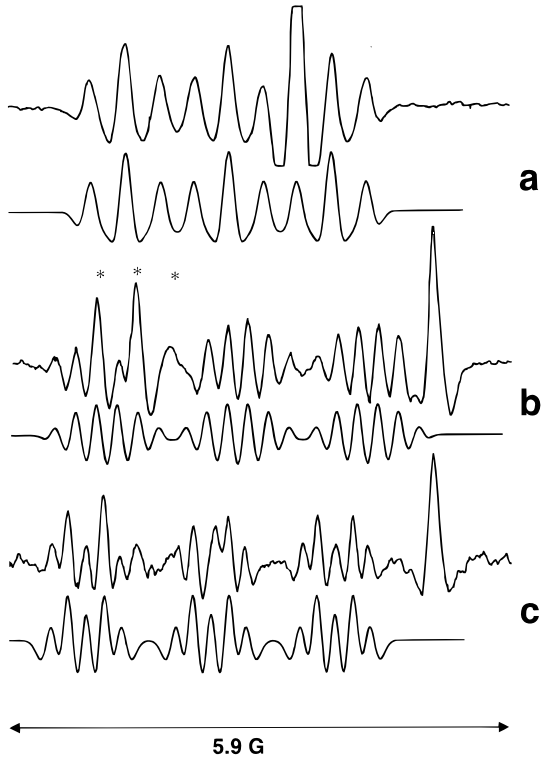

Figure 7. Partial second-derivative spectra of the radicals $RCH_2NO_2^{\bullet-}$ formed in spin-trapping experiments with 8 mM CH_3NO_2 at pH 12: (a) 200 mM NH_3; (b) 100 mM methylamine; and (c) 50 mM glycine. In panel a, the line group is near the center of the low-field CH_2 triplet, and the strong line is that of the $^{\bullet}OH$ adduct. In panels b and c, the groups are at the low-field end of the spectrum, and the strong line is from $CH_3NO_2^{\bullet-}$. In each case, the experimental spectrum is above, and a section of the synthesized spectrum with the parameters of Table 4 is below. Some extra, weaker lines are also superimposed in panels b and c. The asterisks in panel b denote lines attributed to the spectrum of the $^{\bullet}CH_2NH_2$ adduct.

Spin Trapping. As a final attempt at demonstrating the presence of aminyl radicals, spin-trapping experiments with the *aci*-anion form of nitromethane ($H_2C{=}NO_2^-$)[29,30] were performed using steady-state, in situ radiolysis with a flowing solution. As mentioned above, no aminyl radicals, $HN^{\bullet}-CH_2-CO_2^-$, were reported in spin-trapping experiments with the spin trap 5,5-dimethyl-1-pyrroline-*N*-oxide.[12] However, nitromethane has been used successfully to trap $^{\bullet}NH_2$.[31] Figure 7 shows traces obtained with N_2O-saturated solutions of ammonia (Figure 7a), methylamine (Figure 7b), and glycine (Figure 7c) with 8 mM nitromethane at pH 12. In each case, ESR lines of a radical attributable to the adduct of an N-centered radical can be seen. In addition, ESR lines from $CH_3NO_2^{\bullet-}$ are seen as a result of competition with N_2O for e_{aq}^-; there are also lines from the $^{\bullet}OH$ adduct of the *aci*-anion of nitromethane. The ESR parameters are shown in Table 4.

The three spectra in Figure 7 all show splittings from the H and N nuclei in the $-CH_2NO_2^-$ moiety and, in addition, splittings from some nuclei in the added fragments. The spectrum of the adduct of $^{\bullet}NH_2$ is uncomplicated, as found before.[31] The aminyl-radical adducts obtained with methylamine and glycine do not show triplets for the CH_2 protons of the $-CH_2NO_2^-$ moiety. Instead, a pair of line groups is found that can be interpreted as the outer lines of that triplet. Our explanation is that the central line group is broadened by slow

TABLE 4: ESR Parameters for Nitromethane Adducts, $RCH_2NO_2^{\bullet -}$[a]

radical trapped, R	a_N	a_H(CH)	a'_N	a_H(NH)	a_H(CH′)	g
$^{\bullet}NH_2$	26.12	9.18	1.21	0.41(2)		2.005 08
$H_3CN^{\bullet}H$	25.05	9.23	1.53	0.48	0.24(3)	2.005 09
$^{-}O_2CCH_2N^{\bullet}H$	25.17	9.39	1.47	0.42	0.18(2)	2.005 09
$^{\bullet}CH_2NH_2$	25.26	10.26			0.44(2)	2.005 06

[a] All splittings in gauss.

internal rotation and is too weak to be detected. Such an effect has been seen previously for the adduct of $(CH_3)_2C^{\bullet}-OH$ where the central lines of the CH_2 triplets are considerably broadened but still visible.[30] The parameters in Table 4 correspond with such an interpretation. The small nitrogen splittings of the three aminyl radicals are all similar, and in each case, there is the correct number of small proton splittings from NH and CH protons.

With methylamine, there are also lines that can be ascribed to the adduct of $^{\bullet}CH_2NH_2$. In this case, there is a small 0.44-G triplet of somewhat broadened lines at the center of each of the CH_2 triplets from the $-CH_2NO_2^{-}$ moiety, but the lines from the $^{\bullet}CH_2NH_2$ adduct overlap strongly with those of the aminyl adducts on the ends of the CH_2 triplets. For one such occurrence of these 0.44-G triplets, see Figure 7b, where the lines are marked by asterisks. Although the outer lines are somewhat obscured, as in Figure 7, there are lines at each position that corresponds to the parameters given for this radical.

Somewhat weak lines of a possible corresponding adduct of $H_2N-^{\bullet}CH-CO_2^{-}$ are seen with glycine. These lines overlap those of the aminyl and $^{\bullet}OH$ adducts and are, therefore, only tentatively identified. If the structure of this spectrum is properly understood, a splitting is present from the single CH proton. It is interesting that lines from $H_2N-^{\bullet}CH-CO_2^{-}$ itself are still present in the experiment with glycine, even in the presence of nitromethane; the trapping rate must be very slow for this radical. The radical lifetime before trapping must be over $\approx$100 μs.

It is also noted that no adduct of $^{\bullet}CO_2^{-}$ was seen with glycine. Although this method is not quantitative, the great stability of this latter adduct (making large signals in a steady-state experiment)[32] implies that the yield of $^{\bullet}CO_2^{-}$ under these conditions is very small. The lifetime of the aminyl radicals here is not known but trapping may occur before $^{\bullet}CO_2^{-}$ can be formed. The observance of adducts of the two aminyl radicals clearly demonstrates their formation in the reaction of $^{\bullet}OH$ with methylamine and glycine, although the yield of those radicals was not determined.

Discussion of the Mechanism. The observation of aminomethyl radicals from glycine, in addition to $H_2N-^{\bullet}CH-CO_2^{-}$, differs from the earlier ESR work, which detected only the latter.[5,7−12] The main reason, in the case of the earlier radiolysis experiments,[5] is one of sensitivity, as discussed above. The other experiments[7−12] have similar signal-to-noise ratios (or broad lines limiting resolution) and also might not have detected the somewhat weak lines of aminomethyl radical.

The direct detection of aminomethyl radicals from glycine and their "immediate" formation supports the findings of a recent paper on the oxidation of glycine anions.[4] However, the yield of aminomethyl radicals measured here (29%) is significantly less than the amount inferred from the scavenging experiments (63%).[4] In that work, it was assumed that all rapidly formed reducing radicals came from the decarboxylation of $H_2N^{\bullet +}-CH_2-CO_2^{-}$ radicals. The present work shows clearly that there is also an immediate and direct formation of $H_2N-^{\bullet}CH-CO_2^{-}$ by the attack of $^{\bullet}OH$ on glycine anion. This reaction was not included in the original mechanism.[4] One possibility for the initial attack is a branching of the $^{\bullet}OH$ reaction, part by electron transfer to form $H_2N^{\bullet +}-CH_2-CO_2^{-}$ and part to abstract hydrogen. A second possibility would involve only electron transfer and two paths for loss of a proton from either the NH or the CH positions of $H_2N^{\bullet +}-CH_2-CO_2^{-}$ as well as a parallel path for loss of CO_2.

The yield of reducing radicals measured here, 53% for $H_2N-^{\bullet}CH-CO_2^{-}$ plus 29% for $^{\bullet}CH_2NH_2$ or 82% total, is somewhat higher than the value of 63% from the earlier work. The ratio of the yield of $^{\bullet}CH_2NH_2$ to that of $H_2N-^{\bullet}CH-CO_2^{-}$ is comparable with the value from new scavenging experiments using a scavenger that is more discriminating in its reactions with reducing radicals than $MV^{2+\bullet}$.[33]

The presence of aminyl radicals from glycine and methylamine is clearly shown by the spin-trapping experiments. The most likely reason for the failure to detect these radicals in the time-resolved experiments is that the ESR lines of this species are broader than those of the other radicals and, consequently, are too weak to be detected. Alternatively, the lifetime of these radicals might be very short, but this possibility is believed to be less likely on the basis of the simulation. Thus, the absence of direct ESR evidence for aminyl radicals presents no inconsistency with this aspect of the published scheme,[4] and it is likely that the deficit in $^{\bullet}OH$ yield measured for methylamine and glycine does correspond to formation of the aminyl radicals.

The recent scheme[4] had the attraction that it appeared to account for the CO_2 yields while still matching the yields of aminomethyl at low (1−5 mM) glycine concentrations in the absence of large quantities of proton donors. It is not clear, at this time, how relevant the current findings are to the questions of CO_2 yields as there still are open questions about the secondary and possibly subsequent reactions.

The observation of $^{\bullet}CH_2NH_2$ in the experiment with *N*-chloroglycine was somewhat unexpected. Even though there is an excess of glycine (1.5 mM), most of the glycine is in the zwitterionic form at pH 5.8. Both the zwitterion[34] and the acidic[34,35] form of glycine react relatively slowly, on the order of 10^7 M^{-1} s^{-1}, with $^{\bullet}OH$. Furthermore, the reaction between the zwitterion and hydrated electrons (to deaminate) is even slower.[36] To check whether the *N*-chloroglycine could be reacting with the $^{\bullet}OH$ radical, *tert*-butyl alcohol was used to scavenge the $^{\bullet}OH$. When *tert*-butyl alcohol was used, a substantial fraction of the aminomethyl radical signal was still seen. A formation rate of only about 2×10^4 s^{-1} could be expected from the reaction of $^{\bullet}OH$ with the zwitterion form of glycine. Therefore, the signal of $^{\bullet}CH_2NH_2$ must be coming from reactions of the hydrated electron with the *N*-chloroglycine. The most likely sequence of reactions is the formation of the aminyl radical from the reaction of hydrated electrons with the *N*-chloroglycine

$$e_{aq}^{-} + Cl-NH-CH_2-CO_2^{-} \rightarrow HN^{\bullet}-CH_2^{-}\ CO_2^{-} + Cl^{-} \quad (4)$$

followed by a protonation of the aminyl radical to form the zwitterion radical, $H_2N^{\bullet +}-CH_2-CO_2^{-}$

$$HN^{\bullet}-CH_2-CO_2^{-} + BH^{+} \rightarrow H_2N^{\bullet +}-CH_2-CO_2^{-} + B \quad (5)$$

which immediately decarboxylates to form aminomethyl radicals.[4,20]

$$H_2N^{\bullet +}-CH_2-CO_2^{-} \rightarrow {}^{\bullet}CH_2NH_2 + CO_2 \quad (6)$$

There are proton donors (BH^+) available in this solution. In particular, $H_2PO_4^-$, HPO_4^{2-}, and the glycine zwitterion were estimated as being able to protonate the $HN^{\bullet}-CH_2-CO_2^-$ radical with rate constants for eq 5 of 7.4×10^7, 2.5×10^5, and 3.9×10^5 M^{-1} s^{-1}, respectively.[4] Given the concentrations of these species in the solution, the protonation of $HN^{\bullet}-CH_2-CO_2^-$ is fast enough to account for the fast appearance of the aminomethyl radicals with a rate of 4×10^5 s^{-1}. Thus, although there is no direct evidence for the aminyl radicals, $HN^{\bullet}-CH_2-CO_2^-$, this rapid appearance of $^{\bullet}CH_2NH_2$ in this situation can be simply explained if the aminyl radicals are indeed being formed. The corresponding short lifetime of $HN^{\bullet}-CH_2-CO_2^-$ implies that its detection would be possible but that the sensitivity would be reduced. No lines were, in fact, found in the boxcar-mode scan.

The reaction of $^{\bullet}OH$ with glycine zwitterion near pH 5 was also found to produce some aminomethyl radicals, as well as $H_2N-{}^{\bullet}CH-CO_2^-$ and $H_2N-{}^{\bullet}CH-CO_2H$. The formation mechanism is not clear.

Conclusions

Both aminomethyl and $H_2N-{}^{\bullet}CH-CO_2^-$ radicals were identified by TRESR in the oxidation of glycine anion by $^{\bullet}OH$. The rise time of the ESR lines for these two radicals is consistent with the radicals both being formed in the initial reaction of $^{\bullet}OH$ with the glycine anions or in submicrosecond times from the initial products. The yields of these two C-centered radicals relative to the yield of $^{\bullet}OH$ are approximately 29% for aminomethyl radicals and 53% for $H_2N-{}^{\bullet}CH-CO_2^-$. No ESR lines attributable to the aminyl radical, $HN^{\bullet}-CH_2-CO_2^-$, could be directly detected. However, the rapid appearance of aminomethyl radicals in a complementary experiment with hydrated electrons reacting with *N*-chloroglycine could be simply explained based on the formation of $HN^{\bullet}-CH_2-CO_2^-$ radicals in that situation. As a strong confirmation of the presence of aminyl radicals, spin-trapping experiments with nitromethane *aci*-anion were able to detect the presence of N-centered radicals with both methylamine and glycine, but the yields could not be determined.

Acknowledgment. This work was supported by the Office of Basic Energy Sciences of the U.S. Department of Energy. This is Document No. NDRL-4197 from the Notre Dame Radiation Laboratory. The authors thank Drs. M. Bonifačić and I. Carmichael for extensive conversations on this work and Professors K.-D. Asmus and D. A. Armstrong for discussions on ref 4. Mr. P. Wisniowski's assistance with the spin-trapping experiments is also gratefully acknowledged.

References and Notes

(1) Berlett, B.; Stadtman, E. R. *J. Biol. Chem.* **1997**, *272*, 20313−20316.
(2) Schöneich, C. *Exp. Gerontol.* **1999**, *34*, 19−34.
(3) Camaioni, D. M.; Samuels, W. D.; Linehan, J. C.; Sharma, A. K.; Hogan, M. O.; Lilga, M. A.; Clauss, S. A.; Wahl, K. L.; Campbell, J. A. *Organic Tanks Safety Program FY97 Waste Aging Studies*; Pacific Northwest National Laboratory: Richland, WA, 1998.
(4) Bonifačić, M.; Štefanić, I.; Hug, G. L.; Armstrong, D. A.; Asmus, K.-D. *J. Am. Chem. Soc.* **1998**, *120*, 9930−9940.
(5) Neta, P.; Fessenden, R. W. *J. Phys. Chem.* **1971**, *75*, 738−748.
(6) Mönig, J.; Chapman, R.; Asmus, K.-D. *J. Phys. Chem.* **1985**, *89*, 3139−3144.
(7) Taniguchi, H.; Fukui, K.; Ohnishi, S.; Hatano, H.; Hasegawa, H.; Maruyama, T. *J. Phys. Chem.* **1968**, *72*, 1926−1931.
(8) Poupko, R.; Silver, B. L.; Loewenstein, A. *Chem. Commun.* **1968**, 453.
(9) Paul, H.; Fischer, H. *Ber. Bunsen−Ges. Phys. Chem.* **1969**, *73*, 972−980.
(10) Poupko, R.; Loewenstein, A.; Silver, B. L. *J. Am. Chem. Soc.* **1971**, *93*, 580−586.
(11) Paul, H.; Fischer, H. *Helv. Chim. Acta* **1971**, *54*, 485−491.
(12) Taniguchi, H.; Madden, K. P. *J. Phys. Chem. A* **1998**, *102*, 6753−6759.
(13) Verma, N. C.; Fessenden, R. W. *J. Chem. Phys.* **1976**, *65*, 2139−2155.
(14) Fessenden, R. W.; Hornak, J. P.; Venkataraman, B. *J. Chem. Phys.* **1981**, *74*, 3694−3704.
(15) Madden, K. P.; McManus, H. J. D.; Fessenden, R. W. *Rev. Sci. Instrum.* **1994**, *65*, 49−57.
(16) Verma, N. C.; Fessenden, R. W. *J. Chem. Phys.* **1973**, *58*, 2501−2506.
(17) Iacona, C.; Michaut, J. P.; Roncin, J. *J. Chem. Phys.* **1977**, *67*, 5658−5660.
(18) Carrington, A.; McLachlan, A. *Introduction to Magnetic Resonance*; Harper & Row: New York, 1967.
(19) *Chemical Kinetics Simulator 1.0: User's Manual*; IBM Almaden Research Center: San Jose, CA, 1995.
(20) Hug, G. L.; Carmichael, I.; Fessenden, R. W. *J. Chem. Soc., Perkin Trans. 2* **2000**, 907−908.
(21) Logan, S. R. *J. Chem. Soc., Perkin Trans 2* **1989**, 751−754.
(22) Huie, R. E.; Neta, P. *Atmos. Environ.* **1987**, *21*, 1743−1747.
(23) Beckwith, A. L. J. *J. Chem. Soc. B* **1969**, 400−403.
(24) Getoff, N.; Schwörer, F. *Int. J. Radiat. Phys. Chem.* **1971**, *3*, 429−439.
(25) Symons, M. C. R. *J. Chem. Soc., Perkin Trans. 2* **1973**, 797−803.
(26) Hawkins, C. L.; Davies, M. J. *J. Chem. Soc., Perkin Trans. 2* **1998**, 1937−1945.
(27) Fessenden, R. W.; Neta, P. *J. Phys. Chem.* **1972**, *76*, 2857−2859.
(28) Metcalf, W. S. *J. Chem. Soc.* **1942**, 148.
(29) McMillan, M.; Norman, R. O. C. *J. Chem. Soc. B* **1968**, 590−597.
(30) Eiben, K.; Fessenden, R. W. *J. Phys. Chem.* **1968**, *72*, 3387−3393.
(31) Chawla, O. P.; Fessenden, R. W. *J. Phys. Chem.* **1975**, *79*, 2693−2700.
(32) Behar, D.; Fessenden, R. W. *J. Phys. Chem.* **1972**, *76*, 1710−1721.
(33) Asmus, K.-D.; Štefanić, I. Radiation Laboratory, University of Notre Dame; private communication.
(34) Scholes, G.; Shaw, P.; Willson, R. L.; Ebert, M. In *Pulse Radiolysis*; Ebert, M., Keene, J. P., Swallow, A. J, Baxendale, J. H., Eds.; Academic Press: New York, 1965; pp 151−164.
(35) Adams, G. E.; Boag, J. W.; Currant, J.; Michael, B. D. In *Pulse Radiolysis*; Ebert, M., Keene, J. P., Swallow, A. J., Baxendale, J. H., Eds.; Academic Press: New York, 1965; pp 131−143.
(36) Buxton, G. V.; Greenstock, C. L.; Helman, W. P.; Ross, A. B. *J. Phys. Chem. Ref. Data* **1988**, *17*, 513−886.